



Research paper

Impact of numerical modelling of kinematic and static boundary conditions on stability of cold-formed sigma beam

Katarzyna Rzeszut¹, Ilona Szewczak², Patryk Różyło³,
Michał Guminiak⁴

Abstract: The main aim of the study is an assessment of models suitability for steel beams made of thin-walled cold-formed sigma profiles with respect to different numerical descriptions used in buckling analysis. The analyses are carried out for the sigma profile beam with the height of 140 mm and the span of 2.20 m. The Finite Element (FE) numerical models are developed in the Abaqus program. The boundary conditions are introduced in the form of the so-called fork support with the use of displacement limitations. The beams are discretized using S4R shell finite elements with S4R linear and S8R quadratic shape functions. Local and global instability behaviour is investigated using linear buckling analysis and the models are verified by the comparison with theoretical critical bending moment obtained from the analytical formulae based on the Vlasov beam theory of the thin-walled elements. In addition, the engineering analysis of buckling is carried out for a simple shell (plate) model of the separated cross-section flange wall using the Boundary Element Method (BEM). Special attention was paid to critical bending moment calculated on the basis of the Vlasov beam theory, which does not take into account the loss of local stability or contour deformation. Numerical shell FE models are investigated, which enable a multimodal buckling analysis taking into account interactive buckling. The eigenvalues and shape of first three buckling modes for selected numerical models are calculated but the values of critical bending moments are identified basing on the eigenvalue obtained for the first buckling mode.

Keywords: numerical analysis, thin-walled cold-formed steel beam

¹DSc., Poznan University of Technology, Institute of Building Engineering, Marii Skłodowskiej-Curie 5, 60-965 Poznań, Poland, e-mail: katarzyna.rzeszut@put.poznan.pl, ORCID: 0000-0002-7134-608X

²Ph.D., Lublin University of Technology, Faculty of Civil Engineering and Architecture, ul. Nadbystrzycka 38D, 20-618 Lublin, Poland, e-mail: i.szewczak@pollub.pl, ORCID: 0000-0002-4953-0104

³DSc., Lublin University of Technology, Faculty of Mechanical Engineering, ul. Nadbystrzycka 38 D, 20-618 Lublin, Poland, e-mail: p.rozylo@pollub.pl, ORCID: 0000-0003-1997-3235

⁴DSc., Poznan University of Technology, Institute of Structural Analysis, Marii Skłodowskiej-Curie 5, 60-965 Poznań, Poland, e-mail: michal.guminiak@put.poznan.pl, ORCID: 0000-0003-0100-8621

1. Introduction

The history of research on stability of structures is almost 250 years old and it was started in 1759 by Euler, who published a work on buckling in compressed columns. Euler's work was continued by, inter alia, Timoshenko and Vlasov, who formulated a general theory of thin-walled bars in a complex state of stress and elastic loss of stability. Theoretical and experimental studies on the stability of thin-walled elements have shown the shortcomings of classical linear theories and revealed the need for more advanced analyses. It became possible thanks to the development of computer methods and the formulation of a geometric matrix and incremental equations, among the others used in the Finite Element Method [1]. Loss of stability is the most important phenomenon that leads to exceeding of the load capacity of thin-walled metal structures. For this reason, stability conditions are the subject of a large part of design standards and have been introduced into the curriculum in engineer, master and doctoral educational programs. Designers can find practical recommendations in design codes with theoretical and experimental background in the literature [2] how to overcome the problems of instability. In [3] author provides a review of recent developments in research and design practice surrounding the structural use of stainless steel, with an emphasis on structural stability. Whereas, experimental and numerical study of press-braked S690 high strength steel slender channel section columns were conducted in [4]. The special attention was focused on local–flexural interactive buckling. Professional computer programs supporting design of steel structures implement many of these recommendations. However, modern cold-formed steel structures gave rise to new stability problems [5, 6]. In engineering practice two classes of stability problems of cold-formed members have been distinguished. The first of them the global stability is analysed according to Vlasov's theory, which takes into account torsion of the bar, assuming a non-deformable contour. The second class concerns the theory of post-critical load capacity taking into account the local stability of walls. When assessing the load-bearing capacity of civil engineering structures, it may be dangerous to consider these two classes of problems separately. Therefore, when assessing the load-bearing capacity of the elements according to Vlasov's theory, the influence of wall stability should be additionally investigated in accordance with the plate theory as the so called effective length concept proposed by Karman [7]. Much software for computer aided design of metal structures contains ready-to-use procedures for taking into account the influence of instability problems on the structure capacity. However, the phenomenon of stability is so complex that a routine approach to the design of thin-walled structures, as proposed by professional computer programs, can be dangerous or can lead to uneconomical projects. Application of thin-walled cold-formed sections and welded I sections with slender webs increased the importance of local instability phenomena which often appeared at a similar load level as global instability. The case when two or more different modes in stability and dynamic analyses are associated with the same or similar eigenvalues is termed a bimodal or multimodal solution. Designers' concern is that these solutions are very sensitive to imperfections [8]. Design codes contain recommendations with respect to global, local and distortional buckling, which can be taken into account separately. There is definitely not so much information about interactive buckling. Therefore

the question of the reliability of buckling resistance assessment of steel beams is still an unresolved issue. The study of this problem may be of interest to design engineers. Moreover, the problem becomes more complicated when there is a need to define the critical moment for symmetrical sections, where the axis of symmetry is the weaker one, e.g. channels or sigma sections [9]. The Polish standard PN-90 / B-03200 [10] provides a simplified method of load-bearing capacity and torsion analysis of beams made of channel sections (C cross-section). In the case of no interaction between the bending moment and the shear force, it allows to determine the approximate share of torsion in the stress state of the channel section at approx. 15%. On the other hand, the PN-EN 1993-1-1 standard does not provide any method of determining the critical moment for symmetrical sections, where the axis of symmetry is the weaker axis, and refers the designer to basic knowledge on the strength of materials. The present work involves the suitability assessment of the results of calculations of critical moments for cold-rolled sigma cross-section using analytical formulae based on the Vlasov beam theory, contained in [11–13] and the Finite Element Method (FEM) using the Abaqus program and shell finite elements. In addition, the paper attempts to analyse stability using Boundary Element Method (BEM) for a separate wall of profile.

2. Numerical analysis

2.1. Analytical formulae

The numerical analyses, are carried out for the beam with sigma type open cross-section subjected to transverse external load meeting so call Vlasov beam theory assumptions. According to [12], the formula for the critical moment can be computed using the following formula:

$$(2.1) \quad M_{cr} = \frac{C_b \pi^2 E I_y}{l_e^2} \sqrt{\frac{I_\omega}{I_y}}$$

where: l_e – the lateral-torsional buckling length, I_y – the second moment of area with respect to the main axis of the section, perpendicular to the bending direction, I_ω – the warping constant, C_b – a coefficient depending on the bending moment variation along the bar length.

Note that formula (2.1) is used for the critical moment calculation for I-section (i.e. bi-symmetric), channel (i.e. mono-symmetric) and Z-section (i.e. point symmetric) sections, in the case of bending with respect to weaker axis of symmetry. Moreover, when considering sigma-type sections, it can also be used while the sigma-type sections can be treated as C-sections with a web stiffened by an intermediate folds.

In order to conduct comparative analyzes, the critical bending moment was also determined based on the analytical procedure contained in Annex Z1 to the Polish standard PN 90 / B 03200:

$$(2.2) \quad M_{cr} = \pm A_0 N_y + \sqrt{(A_0 N_y)^2 + B^2 i_3^2 N_y N_z}$$

where: A_0, A_1, A_2, B – are the coefficients depending on boundary conditions and the way of load application, N_y – facular buckling load, N_z – torsional buckling load, i_s – radius of inertia.

2.2. Application of the finite element method

Numerical simulations were performed using FEM in Abaqus software. Moreover, all simulations were carried out based on the solution of the linear structural stability problem, known as the linear buckling analysis – LBA (linear perturbation problem). Linear-buckling is also called eigenvalue buckling (Euler buckling) – it predicts the theoretical buckling strength of an elastic structure. The eigenvalues represent the values of load at which buckling occurs. The eigenvectors define the buckling shapes corresponding to the appropriate eigenvalues. Eigenvalue buckling analysis is generally used to determine the critical buckling loads of stiff structures. Moreover, stiff structures carry their design loads primarily by axial/membrane load, rather than by bending load. The response of this type of structures usually involves very little deformation prior to buckling. During the numerical investigations carried out, the buckling form of the structure was determined, along with the corresponding critical load, based on the minimum potential energy criterion. Numerical analyses made it possible to assess the stability of the structure based on the special relationship. In order to solve the linear eigenvalue problem, a unit load was applied to the properly fixed structure, allowing for the determination of the loss of stability (buckling) form as well as the value of critical load. The critical load value was determined using the well-known general eigenvalue problem:

$$(2.3) \quad (\mathbf{K}^O + \lambda \mathbf{K}^G) \mathbf{U} = 0$$

where: λ is the load multiplier and eigenvector \mathbf{U} represents the buckling mode shapes, \mathbf{K}^O is the linear stiffness matrix, \mathbf{K}^G is the initial geometric matrix. In Eq. (2.3) the proportional loading and linearization of the pre-buckling state was assumed. The critical buckling loads are $\lambda_i^c \mathbf{P}$, where \mathbf{P} is the reference load (the base state).

2.3. Application of the boundary element method

The initial stability problem of the selected plate parts of the structures can be formulated and solved using the Boundary Element Method (BEM). A number of publications were devoted to the plate bending analysis, especially considering the stability problem of plates, e.g. [14], wherein it is worth paying attention to the use of the so-called the Analog Equation Method in combination with the classical Boundary Element Method [15–17].

The complex steel profile can be divided into simple elements – plates, fixed at the edges. It is also assumed, that the considered plate is subjected to in-plane loading, which can have a constant or a linear character along a single plate edge.

The thin plate bending is described by the differential equation:

$$(2.4) \quad D \nabla^4 w = -\bar{p}$$

where: $D = Eh^3/(12(1 - \nu^2))$ is the plate stiffness and

$$(2.5) \quad \bar{p} = N_x \frac{\partial^2 w}{\partial x^2} + 2N_{xy} \frac{\partial^2 w}{\partial x \partial y} + N_y \frac{\partial^2 w}{\partial y^2}$$

is the substitute loading expressed by real in-plane loading components N_x , N_y and N_{xy} .

The solution to the equation (2.4) can be expressed as an integral representation which leads to the following equations [18, 19]:

$$(2.6) \quad c(\mathbf{x}) \cdot w(\mathbf{x}) + \int_{\Gamma} \left[T_n^*(\mathbf{y}, \mathbf{x}) \cdot w(\mathbf{y}) - M_{ns}^*(\mathbf{y}, \mathbf{x}) \frac{dw(\mathbf{y})}{ds} - M_n^*(\mathbf{y}, \mathbf{x}) \cdot \varphi_n(\mathbf{y}) \right] d\Gamma(\mathbf{y}) \\ = \int_{\Gamma} \left[\tilde{T}_n(\mathbf{y}) \cdot w^*(\mathbf{y}, \mathbf{x}) - M_n(\mathbf{y}) \cdot \varphi_n^*(\mathbf{y}, \mathbf{x}) \right] d\Gamma(\mathbf{y}) \\ + \int_{\Omega} \left(N_x \cdot \frac{\partial^2 w}{\partial x^2} + 2N_{xy} \cdot \frac{\partial^2 w}{\partial x \partial y} + N_y \cdot \frac{\partial^2 w}{\partial y^2} \right) \cdot w^*(\mathbf{y}, \mathbf{x}) d\Omega(\mathbf{y})$$

and

$$(2.7) \quad c(\mathbf{x}) \cdot \varphi_n(\mathbf{x}) + \int_{\Gamma} \left[\tilde{T}_n^*(\mathbf{y}, \mathbf{x}) \cdot w(\mathbf{y}) - \bar{M}_{ns}^*(\mathbf{y}, \mathbf{x}) \frac{dw(\mathbf{y})}{ds} - \bar{M}_n^*(\mathbf{y}, \mathbf{x}) \cdot \varphi_n(\mathbf{y}) \right] d\Gamma(\mathbf{y}) \\ = \int_{\Gamma} \left[\tilde{T}_n(\mathbf{y}) \cdot \bar{w}^*(\mathbf{y}, \mathbf{x}) - M_n(\mathbf{y}) \cdot \bar{\varphi}_n^*(\mathbf{y}, \mathbf{x}) \right] \cdot d\Gamma(\mathbf{y}) \\ + \int_{\Omega} \left(N_x \cdot \frac{\partial^2 w}{\partial x^2} + 2N_{xy} \cdot \frac{\partial^2 w}{\partial x \partial y} + N_y \cdot \frac{\partial^2 w}{\partial y^2} \right) \cdot \bar{w}^*(\mathbf{y}, \mathbf{x}) d\Omega(\mathbf{y})$$

with $\tilde{T}_n(\mathbf{y}) = T_n(\mathbf{y}) + R_n(\mathbf{y})$, wherein $\tilde{T}_n(\mathbf{y}) = V_n(\mathbf{y})$ along a boundary far from the corner and $\tilde{T}_n(\mathbf{y}) = R_n(\mathbf{y})$ on a small fragment of the boundary close to the corner [18, 19]. It means that shear forces along the two boundary elements in contact at the corner play the role of a corner reaction which is now distributed continuously along them. In the equations (2.6) and (2.7) the shear force, the bending moment, deflection, the angle of rotation in normal direction and the angle of rotation in tangent direction are present. The angle of rotation in tangent direction is not independent and may be calculated using a plate boundary deflection. Alternatively, the governing integral equations are derived using the Betti's theorem, e.g. [18, 19].

In present formulation the fundamental solution of the biharmonic equation

$$(2.8) \quad \nabla^4 w^*(\mathbf{y}, \mathbf{x}) = \frac{1}{D} \cdot \delta(\mathbf{y}, \mathbf{x})$$

is applied as the Green function $w^*(\mathbf{y}, \mathbf{x}) = \frac{1}{8\pi D} \cdot r^2 \cdot \ln(r)$ for a thin isotropic plate, $r = |\mathbf{y} - \mathbf{x}|$, where δ is the Dirac delta whereas \mathbf{x} and \mathbf{y} denote the source and field points, respectively. The coefficient $c(\mathbf{x})$ present in equations (2.6) and (2.7) is equal to: 1, 0.5

and 0 for \mathbf{x} located inside the plate domain, on the smooth boundary and outside the plate domain, respectively. Finally, after elimination of the boundary variables, the standard eigenvalue problem can be obtained [9, 10]

$$(2.9) \quad \{\mathbf{A} - \tilde{\lambda} \cdot \mathbf{I}\} \cdot \boldsymbol{\kappa} = \mathbf{0}$$

with $\tilde{\lambda} = 1/\lambda$ and $\mathbf{A} = \{\mathbf{G}_{\text{KK}} - (\mathbf{G}_{\text{KB}} - \mathbf{G}_{\text{KS}} \cdot \Delta) \cdot [\mathbf{G}_{\text{BB}} + \mathbf{G}_{\text{BS}}]^{-1} \cdot \mathbf{G}_{\text{BK}}\}$, which allows to obtain eigenmodes according to [9, 10].

3. Numerical examples

3.1. Description of the model

Investigations based on numerical simulations were conducted for thin-walled steel structures. Numerical analyses were performed for sigma thin-walled beams produced by the company Blachy Pruszyński. The test specimens were characterized by the following specific geometric parameters: height – 140 mm, the flange width – 70 mm and the wall thickness – 2.5 mm. The cross-section shape of the tested structures was of sigma type. All the tested thin-walled beams were simply supported with the span of 2.20 m and loaded by uniformly distributed loads. The detailed description of the laboratory tests as well as the laboratory stand is presented in the papers [9, 20]. The test specimen structures were made of steel S350 GD. The material was characterized by specific parameters that were directly implemented into the Abaqus® program, used for series of numerical calculations: Young modulus $E = 201.8$ GPa, Poisson ratio $\nu = 0.282$ and yield stress $f_y = 418.5$ MPa. The numerical models developed for the loss of stability analysis had the necessary boundary conditions to perform a valid linear buckling analysis. Regarding the numerical simulations, two different types of finite elements were used within the numerical models in order to describe the system. The first type of the finite element (FE), was S4R (with linear shape functions, four nodes with reduced integration – FEM shell-l), and the second one – the shell element S8R (with quadratic shape functions, eight nodes – FEM-shell-s). The dimension of the finite elements was assumed as 7.5 mm (in this study, the effect of mesh density was analyzed using 6 mm, 7.5 mm and 9 mm mesh. The differences between the results were negligible, with differences 2%). The boundary conditions were modelled not as physical supports, but as the constraints of the relevant degrees of freedom at selected edges. The supports were modelled in order to depict the fork support. Thus, the supports were defined using the displacement constraints imposed on the partition plane of the steel beam at the support zones (in a distance of 0.4 m from the beam end) as the constrained horizontal displacements U_x at the web and the edge stiffeners well as the constrained vertical displacements U_y at the bottom flange. In the case of regions where boundary conditions were introduced, the constraints were defined only for the degrees of freedom corresponding to displacements and the degrees of freedom corresponding to rotation were left free (Fig. 1). The exact way of developing a new numerical model in the Abaqus program is presented in [21].

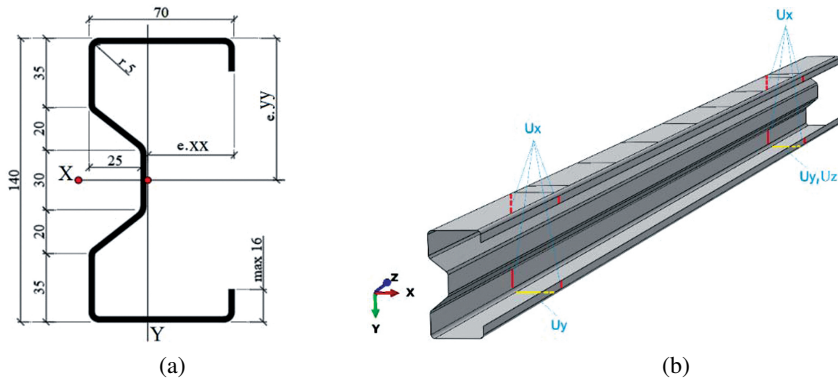


Fig. 1. Numerical model: (a) cross-section geometry $\Sigma 140 \times 70 \times 2.5$; (b) boundary conditions

The conducted numerical simulations were based on Vlasov theory (Numerical models were prepared in order to represent the assumptions of this theory in the most accurate form). Thus, it was assumed that the resultant load should pass through the shear centre of the cross-section of steel sigma profiles and several numerical models were prepared (Fig. 2). The load cases, shown in the figure below, are consistent with Vlasov Theory (except for case c).

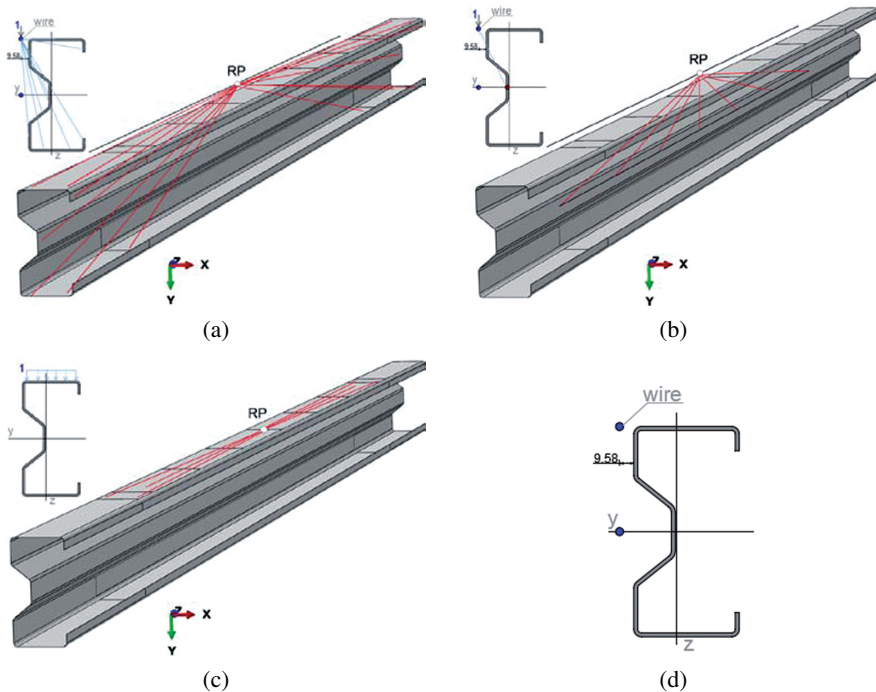


Fig. 2. Load application in numerical model case: (a) V1, (b) V2, (c) V3, (d) WIRE line location

Each of the numerical models developed in Abaqus assumed a different form of load implementation for the structure, appropriately labelled as: V1, V2 and V3. The load cases V1 and V2 as the uniformly distributed load were applied to the hypothetical line, which was located at the level of the upper flange of the cross-section directly above its shear centre. For the V1 load, the reference point has been assigned to a non-deformable specially prepared line “WIRE line” (3D/Discrete Rigid modelling technique) – which made it possible to determine the boundary conditions with the load as the unit force.

Such an approach for the load cases V1, V2 and V3, allowed for a quantitative and qualitative evaluation of the results, and analysis of differences between them depending on the method used. Throughout the analysis, the “Wire line” was a non-deformable element and it was connected to the entire cross-section of the Sigma profile. Moreover, in the case of V2 load type, the non-deformable “Wire line” was treated as a reference point, at which the boundary conditions with the load being the unit force were introduced (the load is transferred uniformly). In the case of V3 load, the uniformly distributed unit loading was applied over the entire width of the upper flange as well as along the length equal to the spacing of supports. The methodology for implementing the load variants described above is shown in Fig. 2.

4. Results of numerical examples

Using Eq. (2.1) (Vlasov beam theory) for the simply supported, beam with the span of 2.20 m and made of $\Sigma 140 \times 2.5$ profile subjected to the uniformly distributed load, the critical moment with the value of 1628 kN·cm was determined. The numerical investigations were carried out for the simplified sigma cross-section geometry with the corners rounding neglected. It is worth noting that the value of the critical bending moment calculated on the basis of the Vlasov beam theory does not take into account the loss of local stability or the contour deformation. On the other hand, these phenomena can be analysed in the FE shell model. For all the developed FE numerical models, a multimodal buckling analysis in Abaqus program was performed. Eigenvalues and shapes for three buckling modes are presented in Fig. 3. It can be observed that the first buckling modes are the combination of global and distortional loss of stability for all considered cases. It should be noted that the type of numerical model used to describe the kinematic and static boundary conditions strongly influences the eigenvalue. On the other hand, the influence of the shape function types is less important. For the second and third buckling mode only local instability is observed. Moreover, the influence of the numerical model and the type of shape function is negligible, and the differences between the linear and quadratic shape function is less than 5%. It can be concluded that the type of FE strongly influences the critical bending moment in case of global or global/distorsional buckling. For the local loss of stability, FEM shell numerical models can be considered as useful and suitable. The analysis of the buckling mode shape leads also to the conclusion that the local buckling is occurred in compressed flange. Therefore, it was considered justified to determine the critical stresses for the separated plate model describing the compressed flange using the Boundary Element

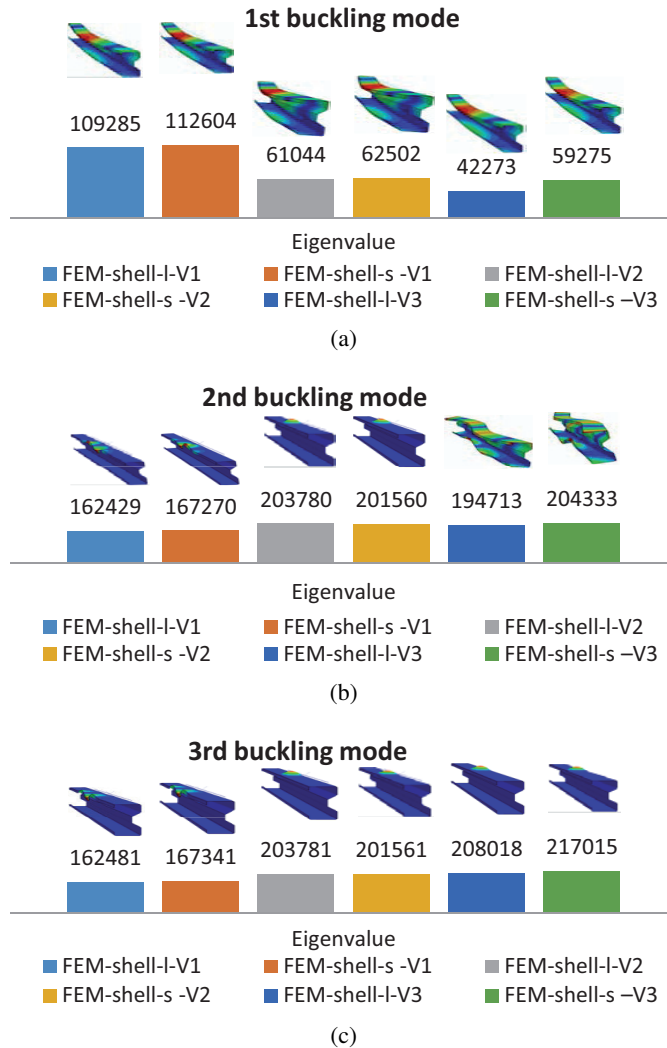


Fig. 3. Shape of buckling mode and eigenvalue for three buckling modes

Method Eq. (2.15). Due to a number of simplifications related to BEM, the stability of the upper flange was analysed assuming two types of kinematic boundary conditions. Namely a cantilever, thus the flange was analysed as an outstand compression wall (BEM-out) and simply supported where the flange was considered as internally compressed (BEM-int). In order to perform a comparison between analytical and FEM or BEM solutions critical stress values were calculated for all the considered numerical analyses (Fig. 4).

One can observe that the lowest values of the critical stress are obtained for the BEM-out model (cantilever). At the same time, the highest values of critical stresses are obtained

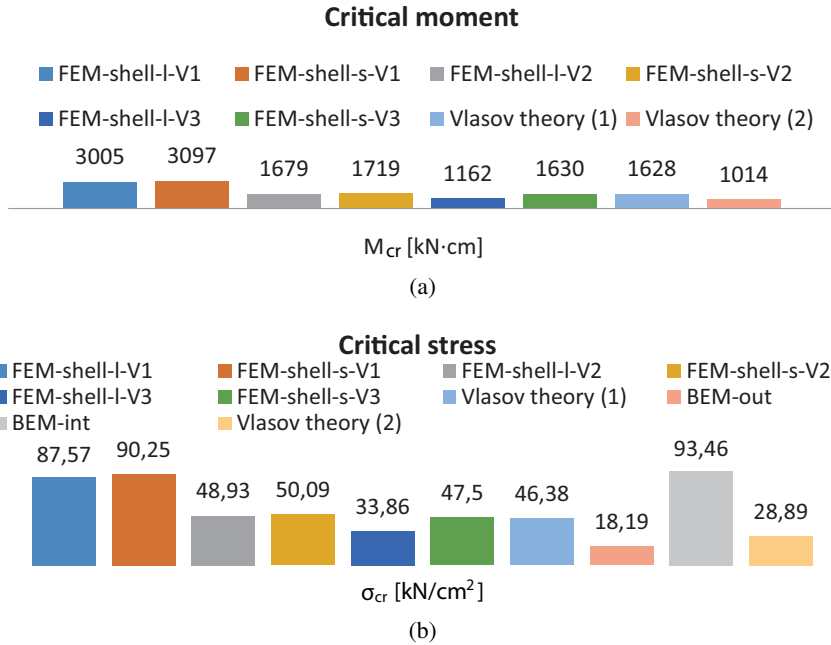


Fig. 4. (a) Critical moment; (b) critical stress for different numerical descriptions

for the BEM-int model (simply supported), which means that designing the structure using this model may be dangerous. The same situation occurs for the case of the critical stresses calculated on the basis of FEM-shell-l-V1 and FEM-shell-s-V1 models. Therefore, these models should be regarded as overestimating and unreliable.

In Fig. 4, the values described as Vlasov theory (1) refer to the value determined according to formula (2.1), and the values of Vlasov theory (2) were determined using the formula (2.2).

On the basis of the obtained results (Fig. 4), it can be concluded that the highest values of the critical stresses are obtained for the shell FEM model with boundary condition according V1, for linear and quadratic shape functions as well. This may be due to the fact that, in model V1, the boundary conditions was imposed on larger areas of the beam. Consequently, these conditions artificially increased the stiffness of the support, so their corresponded more to the rigid than of a simply supported beam. Therefore, the results obtained for these models are similar to BEM-int. It can be noticed that the boundary conditions proposed in the model V2 and V3 with quadratic shape function (FEM-shell-s-V3) very well corresponds to the critical stresses obtained from the analytical solution Vlasov theory (1). On the other hand, model V3 with linear shape function (FEM-shell-l-V3) is similar to analytical solution Vlasov theory (2). It should be noted that in the case of the models V3 (FEM-shell-l-V3 and FEM-shell-s-V3) the high sensitivity to the type of shape function is observed. This may be due to the fact that in this case, boundary

conditions were determined only on one flange of the structure (Fig. 2c). The smaller area of the applied load relative to the structure, could result of obtaining larger discrepancies between the linear and quadratic shape function. This problem was not present in case of V1 and V2 models where the boundary conditions involved larger areas of the beam.

5. Concluding remarks

On the basis of the conducted analyses it is possible to formulate a number of interesting conclusions concerning the numerical modelling in the field of stability analysis of cold-formed steel elements.

First of all, it is clear that the type of the FE, kinematic and static boundary conditions describing the numerical model strongly influence to the value of critical stresses. Buckling analysis in FEM showed that all considered elements undergo to local, distortional and global instability, and in many cases the decisive failure mechanism takes the form of interactive buckling. Unfortunately, as it is known, the theoretical critical bending moment obtained from the analytical closed-form formulae based on the Vlasov beam theory dedicated to the thin-walled elements does not take local or distortional buckling into account. However, in the cases under consideration it can be seen that despite of these limitation the Vlasov theory remains in good accordance with FEM shell model V2 and V3. The comparative analysis presented in Fig. 4 shown that critical moment Vlasov theory (1) is very closed to critical moment obtained for the models V2 and V3 with quadratic shape function (FEM-shell-s-V3). On the other hand critical moment Vlasov theory (2) is close to results obtained by means of the numerical model FEM-shell-I-V3.

Comparing the obtained results of critical moment and critical stress with respect to Vlasov's theory and numerical simulations, it was estimated that the highest discrepancy of the results concerns the numerical models designated as V1 – which may have resulted from coupling the reference point belonging to the reference line to the entire beam profile (which was not the case for models V2 and V3). It was also demonstrated that for local buckling, it is sufficient to analyse the single wall of the cross-section – the one with the greatest plate slenderness. With reference to the buckling results (Fig. 3), it was observed that the first buckling form of the structure for all cases under consideration showed the most probable form of buckling of the structure to occur. The critical load values for the first buckling form are in some cases even several times lower than the critical load for the 2nd and 3rd buckling forms. In this work, due to some BEM simplification the compressed flange was consider only as an outstand or internal wall, while in reality there are semi-rigid support conditions. That is why only the upper and lower estimates of the critical stresses were obtained. Such an analysis was performed for the compressed flange treated as a cantilever wall using BEM. On the other hand it should be emphasized that numerical *FEM-shell-I-V3* model which reflect the real engineering conditions of external load application simultaneously enables multimodal buckling analysis, thus taking into account local, distortional and global buckling and provides reliable values of critical stresses. That is why this model should be regarded as the most suitable one.

Funding

This paper was financially supported by Lublin University of Technology: FN15/ILT/2020 and Poznan University of Technology: 0412/SBAD/0060.

References

- [1] O.C. Zienkiewicz, *The finite element method in engineering science*. London: McGraw Hill, 1977.
- [2] Z. Waszczyszyn, C. Cichoń, and M. Radwańska, *Stability of Structures by Finite Element Methods*. Amsterdam: Elsevier, 1994.
- [3] L. Gardner, “Stability and design of stainless steel structures – Review and outlook”, *Thin-Walled Structures*, vol. 141, pp. 208–216, 2019, doi: [10.1016/j.tws.2019.04.019](https://doi.org/10.1016/j.tws.2019.04.019).
- [4] L. Zhang and O. Zhao, “Experimental and numerical study of press-braked S690 high strength steel slender channel section columns prone to local–flexural interactive buckling”, *Engineering Structures*, vol. 264, art. no. 114468, 2022, doi: [10.1016/j.engstruct.2022.114468](https://doi.org/10.1016/j.engstruct.2022.114468).
- [5] D. Dubina, D. Goina, M. Georgescu, V. Ungureanu, and R. Zaharia, “Recent research on stability analysis of thin-walled cold-formed steel members”, *Journal of Constructional Steel Research*, vol. 46, no. 103, pp. 172–173, 1998.
- [6] C. Szymczak, “Sensitivity analysis of thin-walled members, problems and applications”, *Thin-Walled Structures*, vol. 41, no. 2-3, pp. 271–290, 2003, doi: [10.1016/S0263-8231\(02\)00091-5](https://doi.org/10.1016/S0263-8231(02)00091-5).
- [7] T. Karman, E.E. Sechler, and L.H. Donnel, “Strength of thin plates in compression”, *Transactions of the American Society of Mechanical Engineers*, vol. 54, pp. 53–57, 1932.
- [8] A. Garstecki and K. Rzeszut, “Modeling of initial geometrical imperfections in stability analysis of thin-walled structures”, *Journal of Theoretical and Applied Mechanics*, vol. 47, no. 3, pp. 667–684, 2009.
- [9] K. Rzeszut, I. Szweczek, and P. Różyło, “Issues of thin-walled sigma beams strengthened by CFRP tape in context of experimental and numerical study”, *Engineering Transaction*, vol. 66, no. 1, pp. 79–91, 2018.
- [10] PN-90/B-03200 Steel structures-static calculations and design (in Polish).
- [11] American Iron and Steel Institute, *Specification for the design of cold-formed steel structural*. 1996.
- [12] J. Bródka, M. Broniewicz and M. Giżejowski, *Cold-formed profiles. Designer handbook*. Poland: PWT, 2006.
- [13] R. Szczerba, “Load capacity and stability of steel C-section beams”, *Civil Engineering and Architecture*, vol. 12, no. 2, pp. 283–290, 2013 (in Polish).
- [14] G. Shi, “Flexural vibration and buckling analysis of orthotropic plates by the boundary element method”, *International Journal of Solids and Structures*, vol. 26, no. 12, pp. 1351–1370, 1990, doi: [10.1016/0020-7683\(90\)90083-8](https://doi.org/10.1016/0020-7683(90)90083-8).
- [15] N. Babouskos and J.T. Katsikadelis, “Flutter instability of damped plates under combined conservative and nonconservative loads”, *Archive of Applied Mechanics*, vol. 79, pp. 541–556, 2009.
- [16] B. Chinnaboon, S. Chucheepsakul, and J.T. Katsikadelis, “A BEM-based meshless method for buckling analysis of elastic plates with various boundary conditions”, *International Journal of Structural Stability and Dynamics*, vol. 7, no. 1, pp. 81–89, 2007.
- [17] J.T. Katsikadelis and N.G. Babouskos, “Nonlinear flutter instability of thin damped plates: A solution by the analog equation method”, *Journal of Mechanics of Materials and Structures*, vol. 4, no. 7-8, pp. 1395–1414, 2009, doi: [10.2140/jomms.2009.4.1395](https://doi.org/10.2140/jomms.2009.4.1395).
- [18] M. Guminiak, “An alternative approach of initial stability analysis of Kirchhoff plates by the boundary element method”, *Engineering Transactions*, vol. 62, no. 1, pp. 33–59, 2014.
- [19] M. Guminiak, *The boundary element method in analysis of plates*. Poznan: Poznan University of Technology Publishing House, 2016.
- [20] K. Rzeszut and I. Szweczek, “Experimental studies of sigma thin-walled beams strengthen by CFRP Tapes”, *International Journal of Civil, Environmental, Structural, Construction and Architectural Engineering*, vol. 11, no. 7, pp. 888–895, 2017, doi: [10.5281/zenodo.1131171](https://doi.org/10.5281/zenodo.1131171).

[21] B. Kawecki, "Guidelines for FEM modelling of wood-CFRP beams using ABAQUS", *Archives of Civil Engineering*, vol. 67, no. 4, pp. 175–191, 2021, doi: [10.24425/ace.2021.138493](https://doi.org/10.24425/ace.2021.138493).

Ocena efektywności różnych modeli numerycznych do wyznaczania momentów krytycznych belek sigma profilowanych na zimno

Słowa kluczowe: analiza numeryczna; cienkościenna belka stalowa, profilowanie na zimno;

Streszczenie:

Głównym celem pracy jest ocena przydatności modeli numerycznych belek stalowych wykonanych z cienkościennego profilu sigma formowanego na zimno z uwzględnieniem różnych opisów numerycznych pod kątem analizy wyboczenia. Analizy prowadzone są dla belki o profilu sigma o wysokości 140 mm i rozpiętości 2,20 m. Modele numeryczne Metody Elementów Skończonych (MES) są opracowywane w programie Abaqus. Warunki brzegowe modelowane są w postaci tzw. podpory widełkowej z wykorzystaniem ograniczeń przemieszczeń. Belki modelowane są przy użyciu powłokowego elementu skończonego S4R z liniową lub kwadratową funkcją kształtu. Utrata stateczności lokalnej i globalnej jest badana za pomocą liniowej analizy wyboczeniowej i jest weryfikowana przez porównanie z teoretycznym krytycznym momentem zginającym uzyskanym z analitycznych wzorów opartych na tzw. teorii belek Własowa, dedykowanej dla elementów cienkościennych. Dodatkowo dla prostego modelu powłokowego (płytkowego), dla wydzielonej części przekroju w postaci ścianki (pas lub środek) przeprowadzana jest analiza wyboczeniowa z wykorzystaniem Metody Elementów Brzegowych (MEB). Prowadzona jest również dyskusja dotycząca uproszczeń geometrycznych w przekroju sigma zgodnie z założeniami teoretycznymi. Szczególną uwagę zwrócono na krytyczny moment zginający obliczony na podstawie belkowej teorii Własowa, która nie uwzględnia utraty stateczności lokalnej ani deformacji konturu. Z drugiej strony badane są numeryczne modele powłokowe MES i MEB, które umożliwiają multimodalną analizę wyboczeniową z uwzględnieniem wyboczenia interaktywnego. W artykule wartość własna i kształt postaci wyboczeniowych dla wybranych modeli numerycznych są obliczane dla trzech pierwszych postaci wyboczeniowych, natomiast wartości krytyczne momentów zginających są identyfikowane na podstawie wartości własnej otrzymanej dla pierwszej postaci wyboczeniowej.

Received: 2022-09-21, Revised: 2022-10-18